JACS
JOURNAL OF THE AMERICAN CHEMICAL SOCIETY
Article
pubs.acs.org/JACS

Understanding the Role of Aqueous Solution Speciation and Its Application to the Directed Syntheses of Complex Oxidic Zr Chlorides and Sulfates

Yung-Jin Hu,[†] Karah E. Knope,[†] S. Skanthakumar,[†] Mercouri G. Kanatzidis,[‡] John F. Mitchell,[‡] and L. Soderholm*,[†]

[†]Chemical Sciences and Engineering Division, [‡]Materials Science Division, Argonne National Laboratory, 9700 South Cass Avenue, Argonne, Illinois 60439, United States

Supporting Information

ABSTRACT: The lack of an in-depth understanding of solution-phase speciation and its relationship to solid-state phase formation is a grand challenge in synthesis science. It has severely limited the ability of inorganic chemists to predict or rationalize the formation of compounds from solutions. The need to investigate mechanisms that underlie self-assembly has motivated this study of aqueous Zr-sulfate chemistry as a model system, with the goal of understanding the structures of oligomeric clusters present in solution. We used high-energy X-ray scattering (HEXS) data to quantify Zr correlations in a series of solutions as a function of sulfate concentration. The pair distribution function (PDF) from the sulfate-free sample reveals that the average oligomeric Zr moiety is larger than the tetrameric building unit, $[Zr_4(OH)_8(H_2O)_{16}]^{8+}$, generally understood to dominate its solution speciation. At sulfate concentrations greater than 1 m (molal), bidentate sulfate is observed, a coordination not seen in $Zr(SO_4)_2{\cdot}4H_2O$ (**2**), which forms upon evaporation. Also seen in solution are correlations consistent with sulfate-bridged Zr dimers and the higher-order oligomers seen in **2**. At intermediate sulfate concentrations there are correlations consistent with large Zr hydroxo-/oxo-bridged clusters. Crystals of $[Zr_{18}(OH)_{26}O_{20}(H_2O)_{23.2}(SO_4)_{12.7}]Cl_{0.6}{\cdot}nH_2O$ (**3**) precipitate from these solutions. The Raman spectrum of **3** has a peak at 1017 cm^{-1} that can be used as a signature for its presence in solution. Raman studies on deuterated solutions point to the important role of sulfate in the crystallization process. These solution results emphasize the presence of well-defined prenucleation correlations on length scales of <1 nm, often considered to be within the structurally amorphous regime.

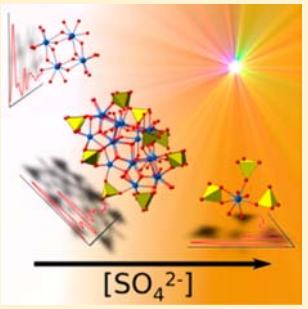

INTRODUCTION

Classical nucleation theory describes the crystallization of inorganic materials from aqueous solution in terms of the additive accumulation of constituent ions. Small clusters form in this manner from stochastic processes of growth and redissolution until they reach a critical size, which depends on a competitive balance between an unfavorable surface energy contribution and a favorable crystal-lattice term, after which further growth is described in terms of ripening processes.[1] Recent work, largely centered on biomineralization, has begun to focus on prenucleation as an important step in crystallization, the details of which can play a fundamental role in precipitate composition and structure.[2,3] Central to this approach is the conceptual movement away from describing crystal growth within the construct of bulk thermodynamics and into a regime in which nanometer-scale interactions play a dominant role.[4,5] Much of the focus of ongoing efforts lies in the assembly of the amorphous aggregates present in solution and that serve as building units (BUs) for the crystalline materials.[6] Missing from this progression, in addition to nucleation theory, is information about the composition and internal structure of the amorphous BUs themselves. Do the BUs have well-defined composition and structure? What are their electronic structures and stabilizing factors? What does the term "amorphous" mean within the context of these small BUs? This lack of an in-depth understanding of any correspondence between solution-phase multi-ion BUs or clusters and solid-state speciation—related to mechanisms that underlie self-assembly—has severely limited the ability of inorganic chemists to predict and rationalize product formation *a priori*.

With the overarching goal of moving away from synthesis by trial-and-error, we are interested in understanding the formation of atomic correlations in solution and their influence on subsequent materials formation. To advance this effort, we are interested in quantifying the molecular-scale detail of preformed ionic clusters in melts or solutions and using this information to inform calculations on relative stabilities.[7−9] The impact of such an approach was recently demonstrated through the examination of potassium polysulfide fluxes, in which it was shown that the S_n^{2-} chains present in the melt influence the structures and compositions of precipitating crystalline materials.[10] Aqueous solution studies have also revealed such a correspondence, as exemplified by the study of uranyl silicates

Received: June 4, 2013
Published: August 22, 2013

   dx.doi.org/10.1021/ja405555h | J. Am. Chem. Soc. 2013, 135, 14240−14248

and the identification in solution of a basic uranyl disilicate moiety that can be viewed as a BU of several known mineral phases.[11] In both examples, small changes in solution conditions result in the precipitation of significantly different materials. Such an atomic-level description of the correlations present in solution can thus provide information necessary to understand how to optimize selected clusters—the BUs for targeted materials—and control their reactivity. Herein we use a series of aqueous Zr sulfate solutions to demonstrate how altering conditions changes the ion correlations in aqueous solution, thereby impacting the composition and structure of resulting precipitates.

Aqueous Zr sulfate solutions were chosen for study because slight changes in solution conditions result in the precipitation of several different compounds.[12−18] Zr itself in aqueous solution is a small, tetravalent ion highly prone to hydrolysis, even under very acidic conditions.[19] Zr was originally thought to exist as the mono-oxo zirconyl ion; however, it was subsequently surmised to exist as the hydroxo-bridged tetramer $[Zr_4(OH)_8(H_2O)_{16}]^{8+}$ on the basis of a structurally characterized chloride precipitate.[20] The addition of sulfate to solutions of the tetramer results in a range of solids with extended hydroxo- and sufato-bridged frameworks.[12,14−17,21−23] In an effort to provide some predictive insights into wide-ranging synthetic efforts, Clearfield used known structures to propose the condensation of "fragments", specifically Zr hydroxyl sulfate monomers, dimers, and trimers, through known olation/oxolation chemistry.[24]

Clearfield's hypothesis offers an elegant construct to explain the formation of various solid-state structures, but still there remains a dearth of information supporting the existence and composition of the proposed solution species. Previous metrical studies of zirconyl solution speciation have included X-ray scattering,[25−29] Raman[30] and extended X-ray absorption fine structure (EXAFS) spectroscopies.[31,32] Herein we take advantage of recent advances in high-energy X-ray scattering (HEXS) to quantitatively determine structural correlations in a series of zirconyl solutions to which the sulfate anion is added. HEXS results are coupled with spectroscopic (IR, Raman) and traditional diffraction techniques to follow changes in the speciation of metal clusters as it evolves from hydroxo-bridged species including the tetrameric $[Zr_4(OH)_8(H_2O)_{16}]^{8+}$ unit in the sulfate-free solution to Zr-sulfate moieties in solutions from which $Zr(SO_4)_2(H_2O)_4$ precipitates. Solution and solid-state structures of polynuclear Zr(IV) species and the mononuclear Zr-sulfates that form through disruption of the tetramer via Zr(IV)-sulfate complexation are described. For the sulfate-free solutions, Zr−Zr correlations inconsistent with the sole presence of the μ_2-hydroxy-bridged tetrameric Zr are observed and thus point to the presence of larger Zr clusters under the solution conditions used herein. The addition of sulfate results in polydisperse solution speciation, including a much larger Zr cluster for intermediate sulfate concentrations and dominant bidentate-sulfate complexation at higher concentrations. Solution conditions favoring large Zr oligomers are identified and facilitate the targeted crystal growth of a deca-octanuclear Zr oxohydroxo cluster (Zr: 18mer). Within a broader context, these results on Zr solutions demonstrate that crystalline precipitates provide some information about metal complexes present in the aqueous phase but do not capture some critical details of species equilibria that may serve a critical role in driving precipitate structure. A predictive understanding of inorganic materials design from solutions will need such information to move forward.

EXPERIMENTAL SECTION

Solution Preparation. Several series of Zr-sulfate solutions were prepared, in which parameters including pH, ionic strength, and/or Zr concentrations were specifically controlled. Over the parameter ranges studied there were no significant changes in either HEXS or Raman data, although in some cases the conditions necessary for precipitation changed slightly. Therefore a series of aqueous solutions were chosen for an exhaustive analysis such that the data reported herein are all obtained from this series. It contained 0.4 m (molal) Zr with varying perchlorate and sulfate concentrations, added in the form of $HClO_4$ and H_2SO_4 mineral acids. The series covered the concentration ranges of 0.00−4.00 m perchlorate and 0.00−2.00 m sulfate and was prepared such that 2 equiv of perchloric acid was replaced by 1 equiv of sulfuric acid. This was done to minimize variations in pH across the series and to minimize the effects of changing ionic strength. All concentrations are reported in molal (m) for ease and accuracy in the conversion of solution HEXS data from counts to electrons. For all samples, the measured pHs were slightly negative, and because pH measurements using a glass electrode at such high acid concentrations suffer from systematic errors, they are nominally reported as about zero. Samples were made in 0.50 m steps in perchlorate and 0.25 m steps in sulfate. The samples were prepared by dissolving $ZrOCl_2{\cdot}8H_2O$ (Sigma-Aldrich, ≥99.5%) with appropriate amounts of milli-Q water (18 MΩ), concentrated $HClO_4$ (Fisher Scientific, Optima), and concentrated H_2SO_4 (Fisher Scientific, Optima) solutions. A similar set of sulfate solutions were prepared with hydrochloric acid (Fisher Scientific, Optima) replacing perchloric acid. Background samples were prepared in a similar manner with $ZrOCl_2{\cdot}8H_2O$ replaced with an appropriate amount of concentrated HCl.

Structural Analysis. See Supporting Information (SI) for details.

Raman Spectroscopy. Raman spectra were collected on the Zr perchlorate/sulfate solution series using a Renishaw inVia Raman Microscope with an excitation wavelength of 532 nm at 10−100% laser power. Each spectrum consists of the summation of 100 acquisitions at 1 s exposure time each.

High-Energy X-ray Scattering (HEXS). HEXS data were collected on the series of Zr perchlorate/sulfate solutions, together with their empty holders and background solutions, at the Advanced Photon Source (APS), Argonne National Laboratory on beamline 11-ID-B. HEXS data were collected with an incident-beam energy of 91 keV, corresponding to a wavelength of 0.13702 Å. The experiment was performed in transmission geometry, and the scattered intensity was measured using an amorphous silicon flat panel X-ray detector mounted in a static position ($2\theta = 0°$) at two different distances, providing detection in momentum transfer space across Q from 0.2 to 28 $Å^{-1}$.[33] Data were obtained on room-temperature solutions and were treated as described previously.[11,33−35] Spectra were corrected for background scattering (by subtracting an empty sample holder) and polarization and were normalized to a cross section per formula unit. Background solutions were used to remove correlations not involving Zr.[33,34,36] The reduced, partial $S^{\Delta}(Q)$ were subsequently Fourier transformed to yield partial pair distribution functions (PDF)s, which show only those correlations involving Zr. As presented in the HEXS figures (Figures 1−3) the peaks in the Fourier transform (FT) of the reduced scattering data represent only the correlations involving Zr, specifically including those with complexed species, solvent molecules, and other solute ions.[33]

The peaks in the PDF are fit to Gaussians, the integration of which provides a direct measure of the electron count contributing to the specific Zr correlation. Of special note are the homoleptic Zr−Zr interactions, for which the obtained electron count must be doubled, complicating quantitative peak assignments when there are more than Zr correlations contributing to the measured scattering. Included in the data fitting and shown in the HEXS figures as the green curve is a modified error function (M-erf) representing the onset of disorder inherent in an aqueous solution.[36] Because the disorder details are not

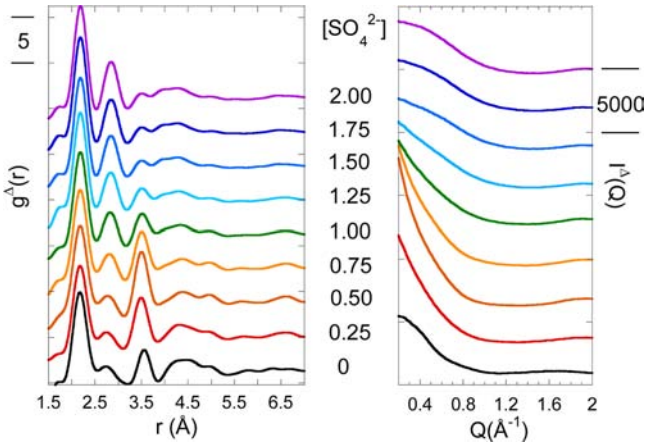

Figure 1. (Left) PDFs constructed from background subtracted HEXS data obtained from a series of 0.4 m Zr^{4+} solutions as a function of sulfate anion concentration. Peaks in the plot represent electron counts in Zr-ion correlations; (Right) Background subtracted, low-*Q*, *I*(*Q*) scattering data over the same series.

uniquely defined using this approach, integrated intensities for peaks that include a contribution from the M-erf (for r > 4.0−4.5 Å) have large errors. The peak positions remain unaffected.

RESULTS AND DISCUSSION

As seen from the scattering results presented in Figure 1, there is evidence for well-defined Zr correlations extending out to distances of 5 Å or more, indicating that there are well- formed aggregates in all measured samples. Also visible from the data is an evolution of solution correlations that change with sulfate concentration. Assignment of specific Zr correlations to each PDF peak must be based on both its position, corresponding to the Zr-ligand distance, and to its intensity, which is directly related to the total number of electrons contributing to the peak. To both assist with and justify our assignments, single crystals that precipitated from the end members of our solution series (sulfate-free and 2.00 m sulfate) were structurally characterized. The structural information obtained in this manner was used to assign features observed in the PDF.

Solid-State Structural description: Compound 1. Compound **1**, $[Zr_4(OH)_8(H_2O)_{16}]Cl_8$, which has been previously structurally characterized,[20] was obtained by evaporation of a sulfate-free, acidic aqueous solution in excess of chloride. A brief discussion of its structural characterization is included herein for comparison with correlations observed from solution HEXS data. Further information is available in the SI.

Compound **1** whose structure comprises isolated $[Zr_4(OH)_8(H_2O)_{16}]^{8+}$ units crystallizes in space group $P\bar{4}2_1c$, with one crystallographically unique Zr atom. The metal is bound to 8 O atoms in its first coordination sphere, arising from 4 waters and 4 bridging OH^- groups, with an average Zr−O distance of 2.18(7) Å. Each Zr is linked to two neighboring Zr via two μ_2-hydroxo-bridges, resulting in the tetramer. All 4 Zr atoms are in the same plane as depicted in Figure 2. As detailed in Table 1, each Zr has two adjacent Zr at distances of 3.547(1) Å, with one additional Zr at 5.015(1) Å corresponding to the tetramer diagonal. Charge balance for the 8+ cationic tetramers is attained by 8 chloride ions, which are not bound directly to the metal but interact via hydrogen bonding with the coordinating waters. There are four such Cl^- ions per Zr at distances of 4.5−4.6 Å.

Table 1. Assignments of Fitted Peaks for the PDF of the Sulfate-Free Solution Shown in Figure 2[a]

peak	center (Å)	intensity (electrons)	assignment	**1**
A	2.18	64(3)	8 O	2.107−2.299 Å
				$4O_H$, 4 O_{water}
B	2.77	18(4)	protons	12 H
C	3.56	51(3)	2.5 Zr[b]	3.5469 Å
				2 Zr
D	4.17	126(6)	∼15 O	18 OH/waters, 6 Cl
	4.4			
	4.65			
E	4.98	56(5)	$Zr_{diagonal}$, Cl(?)	1 Cl (4.998 Å) 1 Zr (5.015 Å)
	5.78		terminal waters	terminal O on adjacent Zr
	6.28		terminal waters	terminal O on diagonal Zr

[a]The HEXS data were obtained from a 0.4 m Zr solution in 4 m perchloric acid. [b]Correlations involving atoms of the same element (in this case Zr−Zr interactions) contribute only 1/2 of their electron count (i.e. one Zr−Zr interaction = 20 electrons).[8,33]

$ZrOCl_2$ in 4 m Perchloric Acid Solution. The PDF pattern shown in Figure 2 exhibits peaks attributable to Zr correlations out to distances of about 7 Å. As detailed in Table 1, the structural information obtained from **1** can be used to assign the peaks observed in the solution PDF. Similar to the

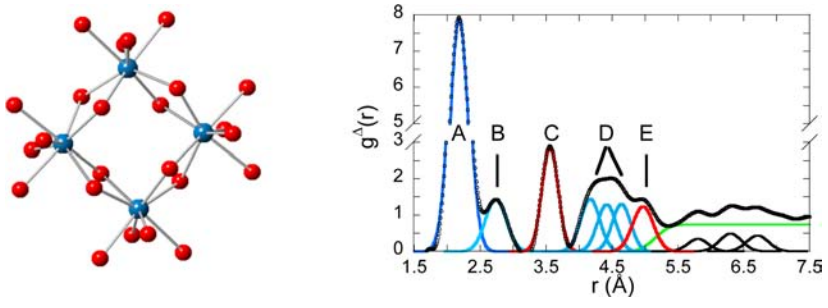

Figure 2. (Left) Isolated tetrameric unit, $[Zr_4(OH)_8(H_2O)_{16}]^{8+}$, seen in compound **1**. Each Zr (blue) is coordinated to 8 oxygen atoms (red) from 4 water molecules and 4 μ_2-hydroxo-bridging groups. (Right) PDF obtained from the sulfate-free member of the acidic, 0.4 m $ZrOCl_2$ solution series. The peaks in the data correspond to correlations with Zr^{4+}. Data are shown as a thick, black line. Gaussian peaks represent fits to the data and are highlighted in blue (O), red (Zr), or black if unassigned. They are labeled in the figure for correspondence to assignments presented in Table 1. Statistically indistinguishable data were obtained using solutions made from the dissolution of $ZrCl_4$ in perchloric acid.

dx.doi.org/10.1021/ja405555h | J. Am. Chem. Soc. 2013, 135, 14240−14248

Table 2. Summary of the Fit to the HEXS Data Shown in Figure 3, Obtained from a 0.4 m $ZrOCl_2$ in 2 m Sulfuric Acid Aqueous Solution[a]

peak	center (Å)	intensity (electrons)	assignment	2
A	2.19	62(3)	8 O	2.1804 Å
				4 O_H, 4 O_{water}
B	2.85	47(3)	3 bidentate S	
C	3.49	22(3)	1.4 monodentate S	3.5339 Å
				4 S
D	3.94	49	6 terminal O from bridging S	3.8810 Å
				4 $O_{terminal\ bridging\ S}$
E	4.98		outer sphere waters?	
F	6.42		$Zr_{S\text{-}bridged}$	4 Zr

[a]The peak assignments are compared with structural features seen in the solid-state structure of $Zr(SO_4)_2(H_2O)_4$ (**2**), which crystallizes from this solution upon evaporation.

solid-state structural result, the Zr^{4+} first coordination sphere is represented by the peak centered at 2.18(2) Å with an intensity corresponding to 64(2) electrons, assigned to eight oxygen atoms. The experimental resolution does not permit the distinction of Zr−O(H) and Zr−O(H_2) distances although it does permit the observation of a peak at 2.7(1) Å, assigned specifically to the protons of the hydroxide and/or water moieties. This result is consistent with previous HEXS studies of dissolved metal ions in which the M−H correlations are observable.[7,35−37] The 18(4) electrons determined from integrating the scattering in this region is slightly more than the 12 electrons expected from the four waters and 4 hydroxides coordinated to Zr in the tetrameric unit, and may indicate some protonation of the ligated waters.

Peak positions in the PDF provide direct evidence for the presence in solution of the tetrameric units observed in the solid-state structure of **1**. Peaks at 3.56 and 4.98 Å are attributable to the hydroxo-bridged Zr−Zr interactions within the tetrameric unit itself. Peaks centered at 4.17 and 4.4 Å are consistent with diagonal hydroxide distances in the tetramer. The presence of a Zr oligmer in solution is further substantiated by the peak in the data at 4.98(4) Å, which is seen in the solid tetramer corresponding to the Zr−Zr diagonal distance of 5.015(1) Å. Also clearly visible in the data are peaks at 5.78 and 6.28 Å, associated with the terminal waters on adjacent (5.78 Å) and diagonal (6.28 Å) Zr. Because of multiple correlations in the regions of interest, it is unclear to what extent Cl^- ion pairs persist in solution, although the 4.65 Å peak may include a contribution from Cl^- ion-paired with the tetramer. The independent interpretation of SAXS data has included bound Cl^- in the description of their solution species.[28] It is noteworthy that, although the tetrameric unit is present in solution, crystals of **1** do not form directly from the solution used for the HEXS experiment unless excess Cl^- is added. Evidence for the preorganized, tetrameric unit in aqueous solution is consistent with previous studies of Raman spectroscopy,[30] small-angle X-ray scattering (SAXS),[27,29] EXAFS,[38,39] and wide-angle X-ray scattering.[25,26] This defines a preponderance of evidence that this tetrameric unit is present under a variety of solution conditions, including higher acidity where hydrolysis is not as favored.

Although the PDF peak positions are consistent with the presence of the tetrameric $[Zr_4(OH)_8(H_2O)_{16}]^{8+}$ unit in solution, the peak intensities reveal a more complicated solution speciation. A detailed analysis of the peak intensities reveals that the data are not consistent with the sole presence of the tetramer. Instead, the fits point to an average cluster size greater than a tetrameric unit. Primary evidence for clusters comes from the peak at 3.56(2) Å, attributed to the adjacent Zr correlations. Either a monodisperse solution of tetramers or a distribution of cluster sizes centered around the tetramer would yield a peak intensity corresponding to two Zr correlations. In contrast, the intensity reveals 2.50(5) Zr associated with this peak. The same result is seen for data obtained from acidic HCl solutions, ruling out the remote possibility of contribution to this correlation from the perchlorate anion. The high correlation number rules out a significant relative presence of smaller monomers, dimers, or trimers which would decrease the average number of Zr−Zr correlations at this distance to below 2 and suggests the presence of more than one oligomeric species. The observation of 2.50(5) Zr−Zr interactions at 3.56(2) Å points to a distribution weighted to tetrameric and larger oligomers. As exemplified by simplified examples, an intensity of 2.5 Zr interactions could arise from a combination of 50% tetramers and 50% pentamers, 75% tetramers and 25% hexamers, or 100% planar octamers.

Literature evidence for these oligomers in aqueous solution comes primarily from structural studies of solid precipitates. Although not previously reported in solution, single crystals composed of hexameric oxo-/hydroxo-bridged Zr clusters have been isolated from aqueous solution and structurally characterized.[40] Similar hexanuclear structures have been reported for a number of other tetravalent metal ions crystallizing from aqueous solution, including Ce^{4+},[41] Th^{4+},[42−44] and U^{4+}.[42] There have been no structures reported for an octameric Zr cluster. An octameric compound with a noncubic structure has been reported for Th^{4+},[43] a much softer ion than Zr, but it has a metal−metal correlation at about 6 Å, a distance with no correlation peak in the PDF, rendering unlikely a similar phase here for Zr^{4+}. The solution occurrence of an octameric unit, in equilibrium with a tetramer, has been previously proposed from the analysis of small-angle X-ray scattering (SAXS) data.[28]

The HEXS data provide metrical evidence that a tetrameric Zr unit, structurally similar to the $[Zr_4(OH)_8(H_2O)_{16}]^{8+}$ cluster seen in the solid, is among at least two preorganized oligomers present in solution. This preorganized cluster is selected to form the crystals of **1** that precipitate upon evaporation. The HEXS data indicate that these BUs are preferentially isolated in the crystal from a disperse solution also containing larger BUs, which may be consumed in the crystallization through a solution equilibrium with the tetramer. This information is relevant for any theoretical efforts aimed at a predictive understanding of Zr^{4+} speciation in aqueous solution.

$Zr(SO_4)_2$ Solution. *Solid-State Structural Description: Compound 2.* Sulfate forms strong complexes with Zr^{4+} and readily displaces OH^- to form sulfato-bridged Zr oligomers. Consequently, there are numerous sulfate compounds that crystallize from aqueous Zr solutions.[13,24,45] For solutions under relatively wide acidic conditions, but with Zr:SO_4 ratios of about 1:2, an apparently stable set of hydrated compounds $Zr(SO_4)_2{\cdot}nH_2O$ are known to form.[13,21,45,46] For use in assigning our HEXS patterns, we crystallized $Zr(SO_4)_2{\cdot}4H_2O$ (**2**) via evaporation of the 2.0 m sulfate solution, the most concentrated in sulfate of those under study here. Details of the structural refinement are provided in the SI; minimal structural details are included herein for ease of comparison.

dx.doi.org/10.1021/ja405555h | J. Am. Chem. Soc. 2013, 135, 14240−14248

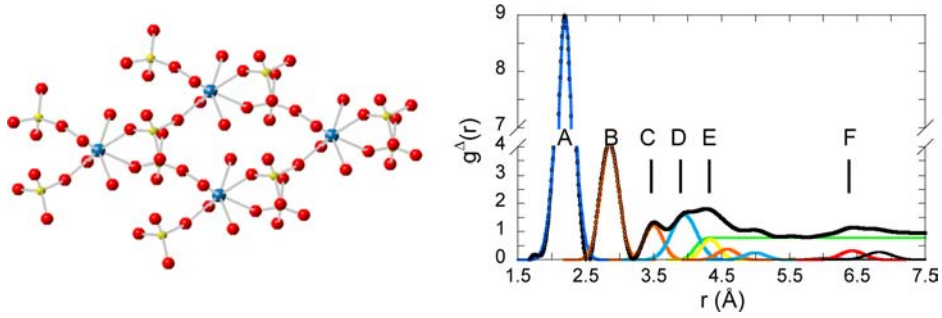

Figure 3. (Left) "Tetrameric" section abstracted from the extended Zr-SO_4 network structure, projected down the *z* axis, found in compound **2**. (Right) PDF obtained by FT of background-subtracted HEXS data from an acidified 0.4 m dissolved $ZrOCl_2$, and 2 m H_2SO_4 solution, out of which crystallizes $Zr(SO_4)_2(H_2O)_4$ (**2**), following evaporation. The peaks in the data correspond to correlations with Zr^{4+}. Data are shown as a thick, black line. Gaussians represent fits to the data and are highlighted in blue (O), red (Zr), or black if unassigned. They are labeled in the figure for correspondence to assignments presented in Table 2.

The compound crystallizes in space group *Fddd*, with one crystallographically unique Zr. The eight Zr-coordinating O atoms, all at a distance of 2.180(1) Å, are associated with four waters and four sulfates that bridge two Zr atoms. The result is layers of composition $Zr(SO_4)_2(H_2O)_4$; hydrogen bonding exists between the layers. The Zr−S distance for the bridging sulfate is 3.534(1) Å, with terminal O distances at 3.881 and 4.356 Å. Four adjacent Zr−Zr, linked by the bridging sulfate groups, are found at 6.435(1) Å. The two diagonal Zr of the pseudo-tetrameric unit depicted in Figure 3 are seen at 5.495(1) Å.

$ZrOCl_2$ in 2.0 m Sulfuric Acid. The HEXS data shown in Figure 3 are obtained from an acidified solution containing 0.4 m dissolved $ZrOCl_2$ in 2 m sulfate, out of which crystallizes $Zr(SO_4)_2{\cdot}4H_2O$ (**2**). Unlike the solution speciation of Zr in perchloric or hydrochloric acids, absent sulfate, the Zr correlations in the presence of sulfate appear markedly different than those expected by comparison with the precipitate structure. The notable difference between Zr solid and solution correlations primarily involves the sulfate coordination motifs. The results of fitting the HEXS data are summarized in Table 2.

Similar to the solution without sulfate, the Zr first coordination sphere is fit with a peak comprising 62(3) electrons, consistent with 8 O at 2.19(2) Å (**B** in Figure 3). The high-*r* shoulder peak at 2.7(1) Å assigned to Zr−H scattering in the sulfate-free sample has shifted to 2.85(3) Å and grown significantly in intensity. The 46(2) electrons under this peak, **B**, are assigned to about 2.2−2.9 sulfur, with bidentate coordination to Zr. Although not present in compound **2**, bidentate-sulfate coordination has been previously observed in the solid state with a Zr−S distance of about 2.96 Å.[15] The uncertainty in the number of coordinating bidentate sulfate anions arises from the uncertainty in the number of Zr−H_{water} correlations contributing to the total electron count. The peak centered at 3.94(3) Å is attributed predominantly to the corresponding bidentate sulfate terminal oxygen atoms.

The small peak at 3.49 Å (**C**) with an intensity of approximately 21 electrons is at a distance consistent with a Zr−S interaction corresponding to a monodentate sulfate or a bridging-bidentate sulfate. For example, the Zr−S (bridging-bidentate) distance is seen in compound **2** at 3.534(1) Å. The correlation of Zr to the bridging-sulfate oxygen atoms is assigned to peak **D**. Peak **E** (4.98 Å) is not unambiguously assigned. Although it could be a diagonal S correlation, it is more likely to be an outer-sphere water. Also present is a significant peak at 6.42 Å (**F**), a distance similar to the distance between adjacent Zr, linked by bridging bidentate sulfate as observed in **2**. There is little evidence for the presence in solution of a diagonal Zr−Zr correlation, seen in the solid sulfate-bridged tetrameric-like unit (Figure 3) at 5.495(1) Å. A peak just discernible above background is seen at 5.54(4) Å.

Solution HEXS data reveal multi-ion aggregates that are candidates for prenucleation BUs. This observation is similar to that seen for the behavior of the sulfate-free sample. Like the solution from which compound **1** precipitates, the sulfate solution out of which compound **2** is formed has much more complex Zr correlations than those observed in the solid. The dominance of the peak at 2.85(3) Å reveals a significant presence of bidentate sulfate coordination to a single Zr, but this species is not seen in the structure of **2**. The presence in solution of a Zr-bidentate sulfate moiety and suggested accompanying equilibria are consistent with the variety of compounds known to precipitate from similar solutions and their dependence on slight changes in solution conditions, including age, temperature, and pH.[13,24,45,46] In addition, the contribution to the scattering from disorder, as expected in solution and modeled with the M-erf, occurs at significantly lower *r* in the sulfate solution than in the solution associated with compound **1**. This behavior suggests that there is more extended ordering about Zr in the solution, absent sulfate, despite the more extended structure of compound **2**.

Zr-Perchlorate/Sulfate Series: Intermediate Sulfate Concentrations. The nonlinear change for selected Zr correlations, visible from intensity trends in the PDFs shown in Figure 4, is contrary to simple expectations for such a series. Most notable is the change in the 3.56(2) Å peak intensity that occurs with increasing sulfate concentration. Increasing sulfate concentrations up to about 0.5 m increase the peak intensities, while sulfate concentrations higher than 0.5 m correlate with decreasing peak intensities. Although expected correlation distances are similar for Zr−S (3.534 Å for Zr−S bridging bidentate) and Zr−Zr (3.55 Å for hydroxy-bridged Zr ions) the scattering pattern is not consistent with simple monodentate sulfate addition to the hydroxo-bridged tetramer. There is a requirement that the model include eight oxygen atoms coordinating to Zr, necessitated by the invariant 2.19 Å peak intensity across the series. Taken together with the bidentate sulfate peak intensities, it is evident that there are increased Zr−Zr interactions contributing to the 3.56 Å peak for the 0.5 m sample.

As shown in Figure 4, the unusual intensity correlation of the 3.56(2) Å peak with sulfate concentration is also seen, albeit

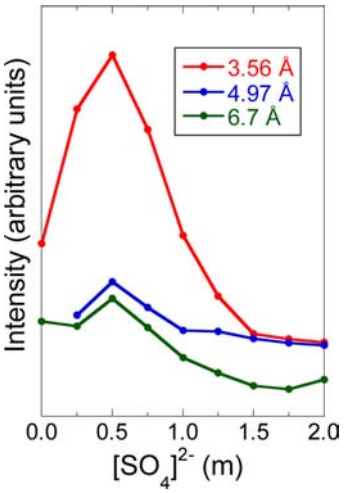

Figure 4. Changes in the integrated intensities of selected PDF peaks (as shown in Figure 1) at 3.56 Å (red), 4.97 Å (blue), and 6.7 Å (green) as a function of total solution sulfate concentration.

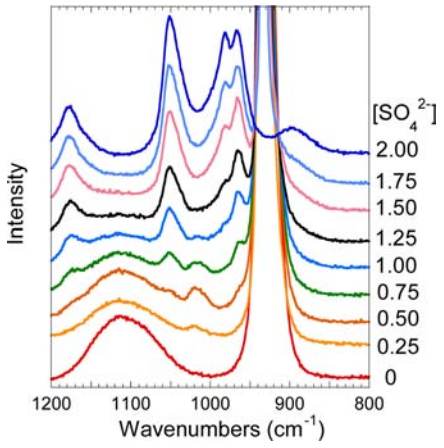

Figure 5. Raman spectra obtained from a series of 0.4 m Zr solutions in $HClO_4/H_2SO_4$. The spectra are offset on the ordinate for ease of viewing.

less dramatically, for two other peaks in the PDF data, at 4.97(4) Å, attributed to diagonal Zr−Zr correlations in the tetrameric unit, and the emergence of a peak at 6.7(1) Å. Overall the changing intensities of peaks at 3.56(2), 4.97(4), and 6.7(1) Å are correlated and increase as sulfate is substituted for perchlorate up to a concentration of 0.5 m in sulfate. For higher concentrations these peaks are seen to systematically and in concert decrease in intensity. This behavior is suggestive of changing average cluster size across the series, increasing with increasing sulfate concentration up to 0.5 m in sulfate, and slowly decreasing with higher sulfate concentration.

Low-Angle X-Ray Scattering Data. Further insights into changes in average cluster size that develop upon the addition of sulfate to the acidic Zr^{4+} solutions come from an inspection of the background-subtracted solution-scattering data depicted in Figure 1 (right panel). These patterns are the low-Q (smaller-angle) data corresponding to the PDFs shown in the left panel. The data exhibit a sample-dependent scattering intensity in the low-Q region, increasing to a maximum intensity for the 0.5 m sample and leveling off with higher sulfate concentrations. The trend of changing low-Q scattering with increasing sulfate concentration follows that seen for the selected PDF correlation peaks shown in Figure 4. The changes observed in the X-ray scattering data across the 0−2 m sulfate series are not consistent with the simple replacement of two hydroxo-bridges in a Zr tetramer with a single, bridging-bidentate sulfate, as suggested by comparing structures of the end-member solid compounds. Instead it appears that there is a large Zr cluster in solution, the average size of which grows with increasing solution sulfate concentration up to about 0.5 m sulfate. Additional sulfate appears to inhibit the formation of larger moieties, eventually replacing the oxolation/olation chemistry with Zr-sulfate complexation.

Raman Spectroscopy. Raman spectra support the observations from scattering data of nonincremental changes in solution speciation for the intermediate samples in the sulfate/perchlorate series. Shown in Figure 5, the Raman spectra can be seen to systematically evolve from perchlorate-dominated features in the absence of sulfate to sulfate-dominated features in the absence of perchlorate. Peak assignments are provided in SI. The exception to this systematic spectral evolution is the peak appearing at 1017 cm^{-1}, which first appears in the 0.25 m sulfate sample, increases in intensity in the 0.5 m, and then decreases with increasing sulfate concentration until it is no longer discernible in the 1.25 m sulfate spectrum. Although not explicitly assigned, trends in its spectral evolution trend with changes in PDF peak correlations, suggesting that the Raman 1017 cm^{-1} peak originates from interactions within a larger cluster.

No well-formed single crystals form from the 0.25−1.25 m sulfate solutions, although a poorly crystalline powder does precipitate from the 0.25 m solution after several days. Not of high quality, an X-ray powder pattern is consistent with a previously reported Zr-deca-octamer (Zr-18mer), $Zr_{18}(OH)_{38.9}O_4(SO_4)_{12.55}(H_2O)_{33}$.[15] No single crystals are prepared from the 0.4 m Zr/0.25 m sulfate in 3.5 m $HClO_4$ solution upon standing; however, decreasing the perchloric acid concentration results in the crystallization of **3**, $[Zr_{18}(OH)_{26}O_{20}(H_2O)_{23.2}(SO_4)_{12.7}]Cl_{0.6}\cdot nH_2O$, after standing in a capped vial for approximately two days. A Raman spectrum of the solid is very similar to that shown in Figure 5 for the 0.25 m sulfate solution. The spectrum includes the peak at 1017 cm^{-1}, which is absent in the spectra from **1** or **2**, indicating that it arises from a structural feature of the Zr-18mer. In the previously reported structural study the material was crystallized out of a $ZrOCl_2$:HCl:H_2SO_4 solution, with relative stoichiometries of 1:0.33:0.6, following aging in a stoppered flask.[15] The Zr-18mer appears to form in solution and act as a BU for a crystalline precipitate over a range of conditions. An important factor appears to be the Zr:SO_4 ratio in the solution, a factor that has previously been suggested to influence the structural composition of these precipitates.[18]

$[Zr_{18}(OH)_{26}O_{20}(H_2O)_{23.2}(SO_4)_{12.7}]Cl_{0.6}\cdot nH_2O$ Structural Study. The structure itself is complex, crystallizing in the space group $P6_3/m$. The Zr-18mers are decorated on the exterior by coordinated sulfate anions, as either bridging or bidentate ligands. None of the sulfate ligands are embedded in the Zr framework shown in the left panel of Figure 6. Adjacent 18mer clusters are linked into chains via bridging bidentate sulfate anions. The clusters are built from 11 crystallographically unique Zr, predominantly eight coordinate although two are seven coordinate. As highlighted in Figure 6, the cluster can be viewed as composed of a central octahedral Zr unit, very similar to the recently reported Zr hexamer,[40] bridged to the remaining Zr through μ_2-hydroxo, μ_3-hydroxo/oxo, and μ_4-oxo

dx.doi.org/10.1021/ja405555h | J. Am. Chem. Soc. 2013, 135, 14240−14248

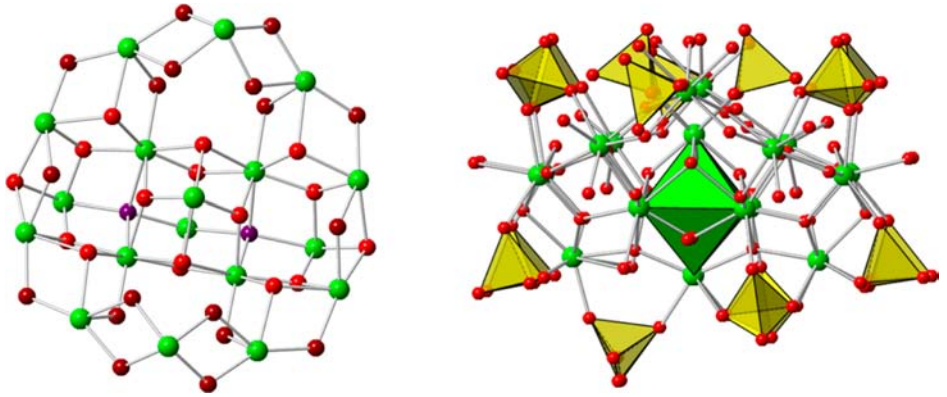

Figure 6. The structure of the 18mer cluster, $[Zr_{18}(OH)_{26}O_{20}(H_2O)_{23.2}(SO_4)_{12.7}]Cl_{0.6}{\cdot}nH_2O$ observed in **3** which was crystallized from a solution similar to the 0.25 sulfate sample in the Zr-sulfate series described in the text. (Left) Decaoctameric (Zr-18mer) cluster. The Zr (green) atoms are linked by μ_2-hydroxo, μ_3-hydroxo, and μ_3-oxo (red), as well as μ_4-oxo (purple) bridges. (Right) View of the same cluster expanded to include the sulfate groups that decorate its surface. This cluster, including the external sulfates, forms the BU for compound **3**. The BUs are linked via two bridging sulfate groups in the structure.

bridges. As suggested by Clearfield,[47] the cluster composition is somewhat consistent with condensation via oxolation/olation chemistry in a manner previously described for higher-valent metal ions in aqueous solution.[48,49]

Solution Behavior of the 18mer BU. Within the context of changing cluster speciation in solution, we are interested in the evolution of the Zr-18mer BU as a function of sulfate concentration. Absent sulfate, HEXS, and Raman data are consistent with tetramers as a solution species, but the HEXS data also require the presence of a larger oligomer, possibly hexameric or stacked octameric species as suggested by independent studies.[28,40] The addition of sulfate favors the growth of the larger clusters, a change that has important implications for directed synthetic applications.[18,50−52] Using the Raman signature peak at 1017 cm^{-1} (shown in Figure 5) as a probe, we have investigated the impact of sulfate addition to an acidic solution containing the Zr tetramer. By using solutions acidified with HCl we were able to identify another peak, at 682 cm^{-1}, previously obscured by a strong perchlorate peak, which can be attributed to the 18mer. Neither peak has been specifically assigned but both are present for solutions containing oligomeric species predominantly larger than tetramers, and from which the 18mer precipitates.

Three deuterated samples were prepared, (1) $ZrOCl_2{\cdot}8H_2O$ was added to an acidic HCl/H_2O solution followed by the addition of sulfate; (2) $ZrOCl_2{\cdot}8H_2O$ was added to an acidic H_2O solution, sulfate was added, followed by the addition of D_2O; (3) $ZrOCl_2{\cdot}8H_2O$ was added to an acidic H_2O/D_2O solution, followed by the addition of sulfate. The Raman spectra from the resulting solutions are shown in Figure 7. For samples in which D_2O was not present upon the addition of sulfate, the peak at 1017 cm^{-1} associated with the 18mer is invariant. However, when the D_2O is present prior to the addition of sulfate (top spectrum in Figure 7) the peak seems to have disappeared. Instead there is a low-energy shoulder to the peak at 682 cm^{-1} that is consistent with a shift to lower energy of the 1017 cm^{-1} peak, as expected for deuteration.

The Raman results provide confirming evidence that sulfate addition is influencing the Zr oligomers present in solution. It is only when D_2O is added before sulfate that there is a shift to lower energy of the 1017 cm^{-1} peak. Moreover, the change indicates that the vibrational mode contributing to the peak involves a proton which becomes nonexchangeable after the addition of sulfate. Such a scenario would be consistent with the growth of a larger cluster that entraps the proton, making it unavailable for exchange.

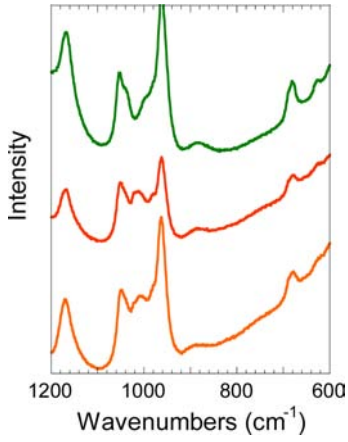

Figure 7. Raman spectra obtained from three samples of 0.4 m $ZrOCl_2{\cdot}8H_2O$ in acidic HCl solutions to which D_2O and 0.5 m sulfate were added. The sole difference is the order in which the D_2O and sulfate were added. (Bottom) $ZrOCl_2{\cdot}8H_2O$ in H_2O to which sulfate was added. (Middle) $ZrOCl_2{\cdot}8H_2O$ in H_2O to which sulfate was added followed by D_2O. (Top) $ZrOCl_2{\cdot}8H_2O$ in H_2O/D_2O to which sulfate was added.

CONCLUSIONS

Synthesis science, defined as the ability to synthesize predicted solid-state phases *a priori*, is in its infancy. Progress along this path hinges on the ability to understand what goes on in the stages preceding crystallization as multiatomic species pre-organize and interconvert in solution. The present study is a step in this direction. The Zr-solution system was selected for study as a model with these aims in mind. As shown schematically in Figure 8, our characterization of Zr speciation in aqueous solution includes the presence of a variety of metal complexes, some of which are not represented in the structures of the crystals that precipitate. Although generally described as amorphous, these small oligomers may be well-defined, correlated structural building units. They exist in complex equilibria that are dependent on solution conditions, including composition and temperature. For example, the quantitative

dx.doi.org/10.1021/ja405555h | J. Am. Chem. Soc. 2013, 135, 14240−14248

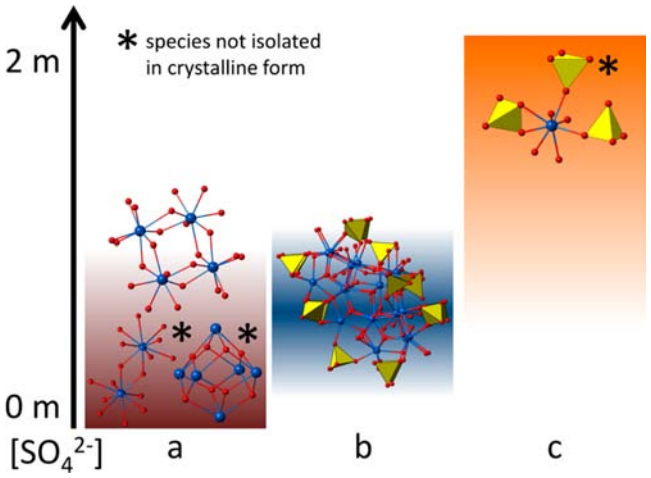

Figure 8. Suggested Zr clusters seen in solution as a function of sulfate concentration. (a) PDF, Raman, and published structures show the presence of a tetramer and a larger cluster as the predominant solution species. The hexameric unit, recently isolated from aqueous solution,[40] is a common structural unit for tetravalent ions.[49] (b) Zr-18mer isolated over a limited sulfate concentration. The presence of other larger oligomers is also possible. (c) Bidentate sulfate complexes of Zr appear to dominate the PDFs for higher sulfate concentrations, although the precipitating structure, **3**, contains only bridging-bidentate units.

analyses of HEXS data obtained from sulfate-free, acidic solutions reveal that the tetrameric $[Zr_4(OH)_8(H_2O)_{16}]^{8+}$ moiety, long understood to be the dominant Zr^{4+} species in solution based on a structural analysis of single-crystal precipitates,[20] shares speciation with larger oligomeric units. These units may include hexameric and/or octameric species, which are in equilibrium with the tetramer. Changing chloride concentration can result in the quantitative precipitation of tetramer as **1**. Only recently have crystals composed of hexameric BUs been isolated from aqueous solution.[40] Further, an octameric BU has only been identified from solution SAXS measurements[28] but has yet to be isolated. We hypothesize that introducing sulfate at low concentrations ($Zr:SO_4 \approx 0.4:0.5$) breaks up some of the hydrolyzed oligomers, providing dimers that, together with remaining intact oligomers, condense to form larger species, as demonstrated by low-angle X-ray scattering, solution HEXS, and by the Zr-18mer that crystallizes from related solutions. Further addition of sulfate destroys the remaining $Zr-(OH)_2-Zr$ units, as evidenced by the absence of a Zr−Zr interaction at 3.56 Å, replacing them with $Zr-SO_4-Zr$ bridging-sulfate moieties. Low-angle X-ray scattering combined with correlations in the PDF patterns confirm that the larger hydroxo-/oxo-bridged Zr clusters are also no longer present. Although $Zr(SO_4)_2{\cdot}4H_2O$ (**2**) forms upon evaporation, the predominant Zr-sulfate coordination at higher anion concentrations involves bidentate ligation. In the solid state, this coordination mode is only seen for two of the sulfate anions decorating the Zr-18mer and is not present in the other sulfates.

This work also points to the importance of anions, particularly in their role as complexing ligands, in the assembly of metal-oxide clusters. It is evident from the solution scattering data as well as the spectroscopic studies that large clusters, on the order of the 18mer, are absent from solution, absent the presence of intermediate sulfate. The evolution of cluster size as a function of sulfate concentration thus raises some critical questions regarding the role of the anion in the formation, stabilization, and precipitation of building units in solution.[55] For example, the extent to which sulfate acts as a structure-directing agent in this system and the prevalence of the deca-octanuclear unit and the extent to which such units exist within other ligand systems such as nitrate, phosphate, or carboxylate remain unclear.

Whereas the single crystals precipitating from solution may provide important structural information about the BUs that precipitate under specific conditions, they may not capture the complex and intricate equilibria involving other oligomers, the presence of which may significantly impact the solution chemistry. The approach described herein that is characterizing solute correlations in solution prior to precipitation provides the basis upon which to develop a deeper understanding of this complex chemistry.

A metrical appreciation for the complexity of solute speciation and their potential equilibria can be critical when relating molecular structure calculations with solution speciation,[43,53] notably when there are unexpected complexes involved in the synthetic pathway.[10] Knowledge of small oligomers and their atomic structures provides an avenue to tie our advancing knowledge of molecular energetics, as provided by theory, with the extensive thermodynamic databases on quantitative equilibria, including that for Zr,[54] which were not developed from a structural perspective. Quantitative structural information about solute speciation and oligomerization provides the linchpin for theory and thermodynamics to play a more direct role in synthesis by design.

Although the Zr oligomers present in the series of solutions under study herein, and sometimes in the solids that precipitate, may be considered amorphous by standard definition, they are not without structural order on the molecular scale. These preformed correlations can have an important role in directing and dictating the structure and properties of materials that form. Therefore, quantifying and tailoring the composition and structures of the preformed BUs in solution points to a more rigorous approach to materials design. The results presented here are relevant to synthesis science and chemistry. The use of powerful *in situ* tools such as HEXS, low-angle X-ray scattering, and Raman spectroscopy in elucidating species prior to compound formation may provide the types of insight necessary to understudy synthetic outcomes and ultimately devise ways to control them.

■ ASSOCIATED CONTENT

Ⓢ Supporting Information

Further characterization information on crystal structures and Raman spectra of synthesized compounds. This material is available free of charge via the Internet at http://pubs.acs.org.

■ AUTHOR INFORMATION

Corresponding Author

ls@anl.gov

Notes

The authors declare no competing financial interest.

■ ACKNOWLEDGMENTS

We thank Dr. Travis H. Bray for technical assistance on related preliminary studies. This work is supported by the U.S. DOE, OBES, Chemical Sciences under Contract DE-AC02-06CH11357. The Advanced Photon Source, used to obtain

the HEXS data described in this study, is supported by the U.S. DOE, OBES, Materials Sciences under the same contract number.

REFERENCES

(1) Debenedetti, P. G. *Metastable Liquids: Concepts and Principles*; Princeton University Press: Princeton, 1996; p 411.
(2) Gower, L. B. *Chem. Rev.* **2008**, *108*, 4551−4627.
(3) Gebauer, D.; Cölfen, H. *Nano Today* **2011**, *6*, 564−584.
(4) Navrotsky, A. *Proc. Natl. Acad. Sci. U.S.A.* **2004**, *101*, 12096−12101.
(5) Demichelis, R.; Raiteri, P.; Gale, J. D.; Quigley, D.; Gebauer, D. *Nat. Commun.* **2011**, *2*, 1604/1−1604/8.
(6) Baumgartner, J.; Dey, A.; Bomans, P. H. H.; Le Coadou, C.; Fratzl, P.; Sommerdijk, N. A. J. M.; Faivre, D. *Nat. Mater.* **2013**, *12*, 310−314.
(7) Wilson, R. E.; Skanthakumar, S.; Sigmon, G.; Burns, P. C.; Soderholm, L. *Inorg. Chem.* **2007**, *46* (7), 2368−2372.
(8) Skanthakumar, S.; Antonio, M. R.; Soderholm, L. *Inorg. Chem.* **2008**, *47*, 4591−4595.
(9) Soderholm, L.; Almond, P. M.; Skanthakumar, S.; Wilson, R. E.; Burns, P. C. *Angew. Chem., Int. Ed.* **2008**, *47*, 493−498.
(10) Shoemaker, D. P.; Chung, D.-Y.; Mitchell, J. F.; Bray, T. H.; Soderholm, L.; Chupas, P. J.; Kanatzidis, M. G. *J. Am. Chem. Soc.* **2012**, *134*, 9456−9463.
(11) Soderholm, L.; Skanthakumar, S.; Gorman-Lewis, D.; Jensen, M. P.; Nagy, K. L. *Geochim. Cosmochim. Acta* **2008**, *72*, 140−150.
(12) McWhan, D. B.; Lundgren, G. *Inorg. Chem.* **1966**, *5*, 284−289.
(13) Bear, I. J.; Mumme, W. G. *Rev. Pure Appl. Chem.* **1971**, *21*, 189−211.
(14) Hansson, M. *Acta Chem. Scand.* **1973**, *27*, 2614−2622.
(15) Squattrito, P. J.; Rudolf, P. R.; Clearfield, A. *Inorg. Chem.* **1987**, *26*, 4240−4244.
(16) El Brahimi, M.; Durand, J.; Cot, L. *Eur. J. Inorg. Chem.* **1988**, *25*, 185−189.
(17) Ahmed, M. A. K.; Fjellag, H.; Kjekshus, A. *Acta Chem. Scand.* **1999**, *53*, 24−33.
(18) Chiavacci, L. A.; Santilli, C. V.; Pulcinelli, S. H.; Bourgaux, C.; Briois, V. *Chem. Mater.* **2004**, *16*, 3995−4004.
(19) Baes, C. E.; Mesmer, R. F. *The Hydrolysis of Cations*; Wiley: New York, 1976.
(20) Clearfield, A.; Vaughan, P. A. *Acta Crystallogr.* **1956**, *9*, 555−8.
(21) Singer, J.; Cromer, D. T. *Acta Crystallogr.* **1959**, *12*, 719−723.
(22) Bear, I. J.; Mumme, W. G. *Acta Crystallogr., Sect. B* **1970**, *27*, 1140−1145.
(23) Bear, I. J.; Mumme, W. G. *Acta Crystallogr., Sect. B* **1970**, *26*, 1125−1131.
(24) Clearfield, A. *Rev. Pure Appl. Chem.* **1964**, *14*, 91−108.
(25) Muha, G. M.; Vaughan, P. A. *J. Chem. Phys.* **1960**, *33*, 194−199.
(26) Aberg, M. *Acta Chem. Scand. B* **1977**, *31*, 171−181.
(27) Toth, L. M.; Lin, J. S.; Felker, L. K. *J. Phys. Chem.* **1991**, *95*, 3106−3108.
(28) Singhal, A.; Toth, L. M.; Lin, J. S.; Affholter, K. *J. Am. Chem. Soc.* **1996**, *118*, 11529−11534.
(29) Hu, M. Z.-C.; Zielke, J. T.; Lin, J. S.; Byers, C. H. *J. Mater. Res.* **1999**, *14*, 103−113.
(30) Baglin, F. G.; Breger, D. *Inorg. Nucl. Chem. Lett.* **1976**, *12*, 173−177.
(31) Kanazhevskii, V. V.; Novgorodov, B. N.; Shmachkova, V. P.; Kotsarenko, N. S.; Kriventsov, V. V.; Kochubey, D. I. *Mendeleev Commun.* **2001**, *6*, 211−212.
(32) Kanazhevskii, V. V.; Shmachkova, V. P.; Kotsarenko, N. S.; Kolomiichuk, V. N.; Kochubei, D. I. *J. Struct. Chem.* **2006**, *47*, 860−868.
(33) Skanthakumar, S.; Soderholm, L. *Mater. Res. Soc. Symp. Proc.* **2006**, *893* (Actinides 2005: Basic Science, Applications and Technology), 411−416.
(34) Soderholm, L.; Skanthakumar, S.; Neuefeind, J. *Anal. Bioanal. Chem.* **2005**, *383*, 48−55.
(35) Skanthakumar, S.; Antonio, M. R.; Wilson, R. E.; Soderholm, L. *Inorg. Chem.* **2007**, *46*, 3485−3491.
(36) Soderholm, L.; Skanthakumar, S.; Wilson, R. E. *J. Phys. Chem. A* **2009**, *113*, 6391−6397.
(37) Wilson, R. E.; Skanthakumar, S.; Burns, P. C.; Soderholm, L. *Angew. Chem., Int. Ed.* **2007**, *46*, 8043−8045.
(38) Cho, H.-R.; Walther, C.; Rothe, J.; Neck, V.; Denecke, M. A.; Dardenne, K.; Fanghanel, T. *Anal. Bioanal. Chem.* **2005**, *383*, 28−40.
(39) Walther, C.; Rothe, J.; Fuss, M.; Buchner, S.; Koltsov, S.; Bergmann, T. *Anal. Bioanal. Chem.* **2007**, *388*, 409−431.
(40) Pan, L.; Heddy, R.; Li, J.; Zheng, C.; Huang, X.-Y.; Tang, X.; Kilpatrick, L. *Inorg. Chem.* **2008**, *47*, 5537−5539.
(41) Lundgren, G. *Ark. Kemi* **1956**, *10*, 183−197.
(42) Takao, S.; Takao, K.; Kraus, W.; Emmerling, F.; Scheinost, A. C.; Bernhard, G.; Hennig, C. *Eur. J. Inorg. Chem.* **2009**, *32*, 4771−4775.
(43) Knope, K. E.; Wilson, R. E.; Vasiliu, M.; Dixon, D. A.; Soderholm, L. *Inorg. Chem.* **2011**, *50*, 9696−9704.
(44) Hennig, C.; Takao, S.; Takao, K.; Weiss, S.; Kraus, W.; Emmerling, F.; Scheinost, A. C. *Dalton Trans.* **2012**, *41*, 12818−12823.
(45) Bear, I. J.; Mumme, W. G. *Acta Crystallogr., Sect. B* **1970**, *26*, 1131−1140.
(46) Bear, I. J.; Mumme, W. G. *Acta Crystallogr., Sect. B* **1969**, *25*, 1558−1566.
(47) Clearfield, A. *J. Mater. Res.* **1990**, *5*, 161−162.
(48) Henry, M.; Jolivet, J.-P.; Livage, J. Aqueous chemistry of metal cations: Hydrolysis, condensation and complexation. In *Struct. Bonding (Berlin)*, **1992**; Vol. *77*, pp 155−206.
(49) Knope, K. E.; Soderholm, L. *Chem. Rev.* **2013**, *113*, 944−994.
(50) Livage, J. *Catal. Today* **1998**, *41*, 3−19.
(51) Park, J. H.; Yoo, Y. B.; Lee, K. H.; Woo, S. J.; Oh, J. Y.; Chae, S. S.; Baik, H. K. *Appl. Mater. Interfac.* **2013**, *5*, 410−417.
(52) Mikkulainen, V.; Leskelä, M.; Ritala, M.; Puurunen, R. L. *J. Appl. Phys.* **2013**, *113*, 021301−021301-101.
(53) Vasiliu, M.; Knope, K. E.; Soderholm, L.; Dixon, D. A. *J. Phys. Chem.* **2012**, *116*, 6917−6926.
(54) Perrone, J.; Illemassene, M. *Chemical Thermodynamics of Zirconium*; Elsevier Science: Amsterdam, 2006; Vol. *8*, p 544.
(55) Hu, Y.-J.; Knope, K. E.; Skanthakumar, S.; Soderholm, L. *Eur. J. Inorg. Chem.* **2013**, *2013*, 4159−4163.